PHYSICAL REVIEW D **85,** 115022 (2012)

Higgs boson production via vectorlike top-partner decays: Diphoton or multilepton plus multijets channels at the LHC

A. Azatov,[1] O. Bondu,[2] A. Falkowski,[3] M. Felcini,[4] S. Gascon-Shotkin,[2] D. K. Ghosh,[5] G. Moreau,[3] A. Y. Rodríguez-Marrero,[4] and S. Sekmen[6]

[1]*Dipartimento di Fisica, Università di Roma "La Sapienza", INFN Sezione, I-00185 Roma, Italy*
[2]*Université de Lyon, Université Claude Bernard Lyon 1, CNRSIN2P3, Institut de Physique Nucléaire de Lyon, F-69622 Villeurbanne Cedex, France*
[3]*Laboratoire de Physique Théorique, Bât. 210, CNRS, Université Paris-sud 11, F-91405 Orsay Cedex, France*
[4]*Instituto de Física de Cantabria (IFCA), CSIC-Universidad de Cantabria, E-39005 Santander, Spain*
[5]*Department of Theoretical Physics, Indian Association for the Cultivation of Science Kolkata, 700 032, India*
[6]*CERN Physics Department, CH-1211 Geneva 23, Switzerland*

(Received 31 March 2012; published 25 June 2012)

We first build a minimal model of vectorlike quarks where the dominant Higgs boson production process at LHC—the gluon fusion—can be significantly suppressed, being motivated by the recent stringent constraints from the search for direct Higgs production over a wide Higgs mass range. Within this model, compatible with the present experimental constraints on direct Higgs searches, we demonstrate that the Higgs (h) production via a heavy vectorlike top-partner (t_2) decay, $pp \to t_2\bar{t}_2$, $t_2 \to th$, allows to discover a Higgs boson at the LHC and measure its mass, through the decay channels $h \to \gamma\gamma$ or $h \to ZZ$. We also comment on the recent hint in LHC data from a possible ~125 GeV Higgs scalar, in the presence of heavy vectorlike top quarks.

DOI: 10.1103/PhysRevD.85.115022 PACS numbers: 12.60.Fr, 14.65.Ha, 14.80.Bn

I. INTRODUCTION

One of the primary goals of the Large Hadron Collider (LHC) is the direct search for the cornerstone of the standard model (SM), namely, the Higgs boson, or for any signal from alternative electroweak symmetry breaking (EWSB) mechanisms. The SM is probably not the ultimate model of nature. It is clear that new channels for Higgs production, that can arise in extensions of the SM, would have profound impact on the discovery of a Higgs boson, while providing insight in the physics beyond the SM. An attractive possibility is the Higgs production in decays of additional heavy colored particles that can be copiously pair produced at the LHC via strong interactions.

Within well-motivated theories beyond the SM, there are some candidates for such new heavy colored states, extra quarks with vectorlike couplings, whose existence is predicted by most of the alternatives to supersymmetry. In this context, to maintain a naturally light Higgs boson, divergent quantum corrections from loops of the top quark are often canceled by top-partner contributions [1–3]. Let us describe important examples here. In the so-called little Higgs scenarios, the vectorlike quarks arise as partners of the SM fields being promoted to larger multiplets. In the composite Higgs [4–8] and composite top [4–9] models, the vectorlike quarks are excited resonances of the bounded states constituting the SM particles. In the extra-dimensional models with (SM) quarks in the bulk, the vectorlike quarks are prevalent as Kaluza-Klein (KK) excitations of those bulk fields [10] like in the gauge-Higgs unification mechanism (see e.g. Ref. [11,12]) or in the Randall-Sundrum (RS) scenario [13–15]—where some of those KK excitations, the so-called custodians, can be as light as a few hundreds of GeV [16–21]. Another example is a gauge coupling unification theory where vectorlike quarks are embedded into the simplest SU(5) representations [22].

Vectorlike quarks with the same electric charge as the up-type quarks are often called top partners (noted t') as these new heavy states mix in general predominantly with the top quark—due to the large top mass and to the related feature that the top quark is in general more intimately connected to ultraviolet physics, like e.g. in composite Higgs models. A t' can also be called a top partner in the sense that it is contained in the same group representation as the top quark with respect to symmetries, like the approximate global symmetry of the little Higgs models [1–3], the gauge unification symmetry [22] or the custodial symmetry of RS versions with bulk matter [16–21] (explaining the SM fermion mass hierarchies [23–39]).

At this level, one must mention that the phenomenology of the search for direct production of vectorlike quarks at the LHC has been studied from a model-independent point of view in Refs. [40–45] but also in specific frameworks such as the little Higgs models (versions sufficiently safe from EW precision constraints) [46–50] or the composite Higgs hypothesis [51,52] and the dual RS context [11,53–58]. These past searches focus generally on the discovery of the vectorlike quarks, rather than using these extra quarks to enhance the discovery and identification potential for other unknown particles such as Higgs scalars.

In relation to Higgs detection, there exist studies utilizing the possible Higgs production through vectorlike quark

decays, as described in the following. Indeed, it is well-known since some time [59,60] that vectorlike quark production could be a copious source of Higgs bosons (a possible Higgs factory). Relatively light Higgs bosons produced from the decay of top partners can be highly boosted and good candidates for analyses based on jet substructure. This method has been applied [61] for a $\sim$130 GeV Higgs decaying to $b\bar{b}$ at the 14 TeV LHC to improve the Higgs identification capability and reduce the background. In the simple model considered there, the t' is a singlet under the $SU(2)_L$ gauge group, which determines the t' couplings and its tree level decays into the Higgs boson and the two EW gauge bosons $t' \to th$, $t' \to tZ$, $t' \to bW$. The top partner can also be singly produced which leads to different final states as compared to the pair production; because of the phase space suppression, the single production becomes competitive with the pair production at a high t' mass, depending upon the considered model (since the involved t' couplings to h, Z^0, $W^{\pm}$ are fixed by the t' quantum numbers) [62]. The reconstruction of the Higgs boson produced in the t' decay, itself singly produced at the 14 TeV LHC, was studied in Ref. [63] assuming the Higgs mass known (to be 12 GeV) and focusing on the channel $h \to b\bar{b}$—with the combinatorial background only. This was performed for a singlet t' in the "Littlest Higgs" model with the asymptotic branching ratio values of the high $m_{t'}$ regime: $B_{t' \to th} = 25\%$, $B_{t' \to tZ} = 25\%$, $B_{t' \to bW} = 50\%$ (from the EW equivalence theorem). Similarly, a vectorlike colored b' state produced at the 14 TeV LHC can act as a Higgs factory thanks to its decay $b' \to bh$. It was shown [22] that a Higgs mass reconstruction can be obtained with a limited accuracy, concentrating on the decay $h \to WW$ ($W \to l\nu$) for $m_h = 200$ GeV and assuming the $m_{b'}$ value to be deduced from a preliminary analysis based on the more appropriate channel $b' \to bZ$. Theoretically, the b' was originating from the upper component of a $SU(2)_L$ doublet so there was no significant channel $b' \to tW$. Higgs mass reconstructions via t' and b' decays were also studied for the 14 TeV LHC, based on a light Higgs decaying to $b\bar{b}$ in the basic models with a unique extra t' and/or a unique extra b' [44].

In the present paper, we use the pair production and decay of a vectorlike top to develop new search strategies for Higgs boson discovery and mass measurements in the $h \to \gamma\gamma$ (diphoton) and $h \to ZZ$ channels. We consider t' masses up to $\sim$800 GeV, so that the t' single productions (involving a model-dependent coupling) are generally subleading compared to the t' pair production not yet significantly suppressed by phase space factors [64]. The original theoretical and illustrative model considered here, including two top partners, is constructed to allow interesting interpretations correlating the indirect (via vectorlike top decay) and direct Higgs production searches at the LHC, as described in the following. A few characteristic parameter sets—with vectorlike top mass in the range between $\sim$400 and 800 GeV—are chosen as benchmark points avoiding too large t' contributions to the Higgs rates (constrained by present LHC data) and simultaneously allowing for significant branching fraction values ($\gtrsim 10\%$) of the vectorlike top decay to the Higgs boson. Assuming the presence at low-energy scales only of extra vectorlike quark multiplets containing some t', we have elaborated a minimal model allowing to strongly suppress the Higgs production via gluon fusion, as compared to the SM. In this simple but nontrivial model, the $gg \to h$ cross section suppression factor possibly reaches values below 10^{-1} at hadron colliders; this is to be put in contrast with the t' representations taken usually in the RS scenario [21,65–69] and with minimal supersymmetric theories for which such a suppression is not possible to obtain (see respectively Ref. [21,65] and Ref. [74]). The chiral case of a fourth quark generation can even only increase considerably the gluon fusion rate. The illustrative minimal t' model suggested here is interesting in the sense that it can easily lead to the following interpretations: for example, a 255 GeV Higgs is excluded in the SM by the present LHC results [75,76] but can still exist in the above minimal SM extension with t' where the reduced Higgs production cross section can be below the LHC upper limits. In other words, the Higgs boson would really be light but not detectable with the present luminosity/energy, via conventional channels. A channel that could then allow the Higgs discovery would be through the t' pair production and decays, as illustrated in this paper. Another possibility is that the slight excess of events observed in data for a Higgs mass hypothesis of $\sim$125 GeV [77,78] is confirmed by the 2012 searches at the LHC. Then the measured Higgs production cross section times branching ratios could certainly be reproduced by the present t' model, given the parameter freedom in this model and its capability of inducing large Higgs rate corrections of both signs. Then investigating this additional Higgs production channel as the t' decay, as discussed here, would of course be relevant, in particular, to confirm the Higgs existence. Finally, in the case of a signal from a heavy Higgs, say above 500 GeV [79] as we will consider here, the same fit of Higgs data would be instructive as a test of the present t' model and similarly the t' decay should be considered as a complementary channel of Higgs production.

II. THE THEORETICAL MODEL

At low scale, let us assume the presence of a unique additional vectorlike quark multiplet including a t' component. Then, irrespective of the representation of this multiplet under the $SU(2)_L$ gauge group (i.e. the t' belongs to a singlet, doublet, ...), the interferences between the next heavier top mass eigenstate t_2 (composed of t, t', t'') and the t_1 ($\equiv$ the physical top quark whose mass is measured) contributions [80] to the triangular loop of the gluon-gluon fusion mechanism will be systematically constructive. This is due to the fact that the physical signs of the Yukawa

coupling and mass insertion involved in this loop—two chirality flips are necessary—will be systematically identical giving rise to a positive product (for t_1 as well as for t_2). Hence, the cross section of the gluon fusion mechanism may be increased or slightly decreased (because of a possible t Yukawa coupling reduction) relatively to the SM case. To get the minimal scenario with only additional vectorlike quark multiplets including t' components able to strongly suppress the gluon fusion, one needs to introduce a first top partner t' in a $SU(2)_L$ doublet as well as a second top partner t'' in a gauge singlet. For simplification, we do not consider the doublet including a b' [81] that would also be exchanged in the triangular loop. So we end up with the doublet $(q_{5/3}, t')$, $q_{5/3}$ being an exotic quark with electric charge $5/3$ and without self-Yukawa coupling (in turn no possible loop exchange). Indeed, with this field content, all the possible generic mass terms and Yukawa couplings appearing in the Lagrangian are,

$$\begin{aligned}\mathcal{L}_{\text{Yuk}} = {} & Y\overline{\begin{pmatrix} t \\ b \end{pmatrix}}_L H^\dagger t_R^c + Y'\overline{\begin{pmatrix} q_{5/3} \\ t' \end{pmatrix}}_L H t_R^c \\ & + Y''\overline{\begin{pmatrix} q_{5/3} \\ t' \end{pmatrix}}_{L/R} H t''_{R/L} + \tilde{Y}\overline{\begin{pmatrix} t \\ b \end{pmatrix}}_L H^\dagger t''_R \\ & + Y_b\overline{\begin{pmatrix} t \\ b \end{pmatrix}}_L H b_R^c + m\bar{t}''_L t_R^c + m'\overline{\begin{pmatrix} q_{5/3} \\ t' \end{pmatrix}}_L \begin{pmatrix} q_{5/3} \\ t' \end{pmatrix}_R \\ & + m''\bar{t}''_L t''_R + \text{H.c.} \end{aligned} \quad (1)$$

where H represents the SM Higgs doublet and L/R the fermion chiralities. By construction, the vectorlike quarks possess same quantum numbers and gauge group representations for the left-handed and right-handed states. We have not written the Yukawa couplings for the first two quark generations as their mixings with the top partners t', t'' are negligible compared to the t-t'-t'' mixing and the CKM mixing angles are typically small, so that the first two quark generations are decoupled from b, t, t', t''. Note that a field redefinition rotating t_R^c and t''_R can allow to eliminate the m term without loss of generality. A last remark is that the Y'' term could be split in two terms with different chiralities and coupling constants. The Lagrangian (1) gives rise, after EWSB, to this top mass matrix:

$$\mathcal{L}_{\text{mass}} = \overline{\begin{pmatrix} t \\ t' \\ t'' \end{pmatrix}}_L \begin{pmatrix} Yv & 0 & \tilde{Y}v \\ Y'v & m' & Y''v \\ m & Y''v & m'' \end{pmatrix} \begin{pmatrix} t^c \\ t' \\ t'' \end{pmatrix}_R + \text{H.c.} \quad (2)$$

with $v \simeq 174$ GeV the SM vacuum expectation value of the Higgs boson. In our notations of Eq. (2), the parameters Y, Y', Y'' and $\tilde{Y}$ contain the whole sign (i.e. the combination of the $SU(2)_L$ contraction signs and Yukawa coupling constant signs). Note that vectorlike fermions do not require EWSB to acquire mass. The nontrivial consequence of the present t', t'' charge assignment choice is the presence of Yukawa terms in the block diagonal matrix of Eq. (2) associated to the top partners [82] (such Yukawa matrix elements would be absent in the first case of a unique top partner). This feature of the mass structure allows strong suppressions of the gluon fusion mechanism. In particular, the own top-partner (t', t'') Yukawa coupling (Y'') sign can be chosen independently of the top (t) Yukawa coupling (Y) sign in order to generate destructive interferences between the top and top-partner loops.

III. t_2 RATES AND DIRECT CONSTRAINTS

We consider here the model described in the previous section, where t', t'' denote the states in the interaction basis while t_1, t_2, and t_3 stand for the mass eigenstates, with $m_{t_3} > m_{t_2} > m_{t_1}$, t_1 being the standard top quark and m_{t_1} its physical mass. We concentrate on the phenomenology of the next-to-lightest top mass eigenstate t_2; the t_3 eigenstate production is subdominant given its larger mass. In a second stage, one could add the contributions to the Higgs production from the t_3 decays like $t_3 \to t_1 h$ or $t_3 \to t_2 Z$.

In Table I, we define our benchmark points by the values of the fundamental parameters—including the Higgs mass m_h—and the corresponding m_{t_2}, m_{t_3} values. These sets of parameters are selected, in particular, to have a large branching fraction $B_{t_2 \to t_1 h}$ enhancing the studied Higgs signal. Note that in the minimal model with a unique doublet $(q_{5/3}, t')$, $B_{t_2 \to bW}$ is negligible compared to $B_{t_2 \to t_1 h}$ and $B_{t_2 \to t_1 Z}$ [44]. For none of the considered benchmark points, the channel $t_2 \to q_{5/3} W$ is open. Table I also provides the theoretical t_2 widths and the $\sigma_{\bar{t}_2 t_2}$ cross sections for the t_2 pair production at LHC computed with the HATHOR program [85] at NNLO. As a comparison, we give also in Table I the expected SM cross sections [86] for Higgs production via gluon fusion, $\sigma^{\text{SM}}_{gg \to h}$. It is physically important to note that the branching ratios $B_{t_2 \to t_1 h}$ and $B_{t_2 \to t_1 Z}$ are not vanishing in contrast with the case of a fourth-generation t' quark so that the observation of such decays (discussed in Sec. VI) would even prove the vectorlike nature of a heavy toplike quark.

Table I presents finally the CMS constraints on the observables $\sigma_{\bar{t}_2 t_2} B^2_{t_2}$ derived from the search for pair production of a heavy toplike quark [75,83,84] (present bounds from ATLAS are less stringent [76,87]). It appears that the corresponding theoretical values, predicted in the models considered here, respect those experimental limits for m_{t_2} as low as $\sim$400 GeV [88]. Increasing theoretically $B_{t_2 \to t_1 h}$, and consequently lowering $B_{t_2 \to t_1 Z}$ and $B_{t_2 \to bW}$, is allowed within these constraints.

Because of these lower limits on m_{t_2} typically around 400 GeV, the t_2 pair production suffers from a significant phase space suppression so that the whole rate for a single Higgs production through the t_2 decay is smaller than for the standard gluon fusion mechanism; there is e.g. a factor of $\sim$10 for point A1 at 14 TeV, as shown the Table I.

TABLE I. Benchmark scenarios in the present t', t'' model, defined by the values of the fundamental parameters, including the Higgs mass, m_h, and the resulting m_{t_2} and m_{t_3} physical masses of the heavy toplike quarks. The cross sections at next-to-next-to-leading order, $\sigma_{\bar{t}_2 t_2}$, for the $pp \to \bar{t}_2 t_2$ process, are shown at $\sqrt{s} = 7$ TeV or 14 TeV, together with the t_2 widths Γ_{t_2} and the t_2 branching fraction values. For comparison, the SM Higgs production cross section values via gluon fusion are also given, together with the ratio $\sigma^{t'}_{gg\to h}/\sigma^{\rm SM}_{gg\to h}$, between the gluon fusion cross section in the present model and in the SM. Furthermore, the next-to-leading-order cross sections for Higgs production in association with a $\bar{t}t$ pair, $\sigma^{t'}_{\bar{t}_1 t_1 h}$, in the present model, are shown for comparison with the $\sigma_{\bar{t}_2 t_2}$ cross sections [the $\sigma^{t'}_{\bar{t}_1 t_1 h}$ values are too small to contribute to the signal, analyzed in this paper, from $\bar{t}_2 t_2$ production, with $t_2 \to th$ decay]. Finally, the LHC upper limits and theoretical predictions for the observables $\sigma_{\bar{t}_2 t_2} B^2_{t_2\to bW}$, $\sigma_{\bar{t}_2 t_2} B^2_{t_2\to t_1 Z}$ are shown just above the last line (the crosses indicate the absence of experimental limit at the associated m_{t_2} values). In the last line the values of the oblique parameters S and T are given [after subtraction of the SM contributions to include only new physics effects]. For the point A1 (A2), we have used the indicated Y'' value for the t''_R coupling and $Y'' = -0.3$ (-1.75) for the t''_L vertex.

Parameter set	A1	A2	B	C	D
$Y/\tilde{Y}$	$-1.43/2$	$1.02/-0.1$	$1.15/0.4$	$1.12/-0.5$	$1.05/-0.3$
Y'/Y''	$1.85/-1$	$1/0.55$	$-1.5/1.6$	$1.1/1.65$	$1.7/1.9$
m/m' (GeV)	0/370	0/675	0/770	0/810	80/1100
m'' (GeV)	510	645	980	850	1100
m_{t_3} (GeV)	722	804	1181	1125	1454
m_{t_2} (GeV)	403	599	626	572	788
m_h (GeV)	125	125	255	320	540
$\sigma^{\rm SM}_{gg\to h}$ (pb) @ 7 TeV	15.31	15.31	3.18	2.25	0.58
$\sigma^{\rm SM}_{gg\to h}$ (pb) @ 14 TeV	49.85	49.85	13.50	10.59	3.85
$\sigma^{t'}_{gg\to h}/\sigma^{\rm SM}_{gg\to h}$	1.27	1.31	0.45	0.40	0.65
$\sigma^{t'}_{\bar{t}_1 t_1 h}$ (pb) @ 7 TeV	0.0194	0.0760	0.0037	0.0016	$7\,10^{-4}$
$\sigma^{t'}_{\bar{t}_1 t_1 h}$ (pb) @ 14 TeV	0.138	0.539	0.036	0.021	0.015
$\sigma_{\bar{t}_2 t_2}$ (pb) @ 7 TeV	1.361	0.0936	0.0709	0.1360	0.0115
$\sigma_{\bar{t}_2 t_2}$ (pb) @ 14 TeV	13.53	1.465	1.164	1.975	0.284
$B_{t_2\to t_1 h}$(%)	62.6	82.1	60.8	13.5	43.0
$B_{t_2\to t_1 Z}$(%)	28.6	14.7	25.0	46.1	40.3
$B_{t_2\to bW}$(%)	8.8	3.2	14.2	40.4	16.6
Γ_{t_2} (GeV)	4.4	3.5	19.8	6.5	8.8
$\sigma_{\bar{t}_2 t_2} B^2_{t_2\to bW}$ (pb)	0.01	$9\,10^{-5}$	0.001	0.022	0.000(3)
LHC bound [83]	<0.26	<0.14	<0.14	<0.16	$\times$
$\sigma_{\bar{t}_2 t_2} B^2_{t_2\to t_1 Z}$ (pb)	0.11	0.002	0.004	0.029	0.002
LHC bound [84]	<0.5	<0.4	<0.4	<0.4	$\times$
S/T	0.05/0.05	0.03/0.03	$-0.01/0.23$	$-0.01/0.30$	$-0.01/0.28$

However, the number of Higgs events issued from the t_2 decay can be significant at 14 TeV with suitable luminosities. This Higgs production channel can thus be an interesting Higgs boson (and t_2) discovery channel, among others, and especially in cases where the gluon fusion mechanism is suppressed by the presence of t', t'' states, as it occurs for instance with point B (see Table I).

IV. CONSTRAINTS FROM THE DIRECT HIGGS BOSON SEARCH

Sets A1/A2—At $m_h = 125$ GeV, all the sensitive channels for searching the Higgs boson at hadron colliders are the decays $h \to \gamma\gamma$, $h \to WW$ (with $W \to \ell\nu$), $h \to ZZ$ (with $Z \to \ell\bar{\ell}$), $h \to \tau\bar{\tau}$ and $h \to b\bar{b}$. The latest bounds on the Higgs boson rates obtained at the LHC read as $\sigma_{gg\to h} B_{h\to\gamma\gamma}/\sigma^{\rm SM}_{gg\to h} B^{\rm SM}_{h\to\gamma\gamma} \lesssim 2$, $\sigma_{gg\to h} B_{h\to WW}/\sigma^{\rm SM}_{gg\to h} \times B^{\rm SM}_{h\to WW} \lesssim 1.30$, $\sigma_{gg\to h} B_{h\to ZZ}/\sigma^{\rm SM}_{gg\to h} B^{\rm SM}_{h\to ZZ} \lesssim 2.2$, $\sigma_{gg\to h} B_{h\to\tau\tau}/\sigma^{\rm SM}_{gg\to h} B^{\rm SM}_{h\to\tau\tau} \lesssim 3.2$ and $\sigma_{gg\to h} B_{h\to bb}/\sigma^{\rm SM}_{gg\to h} B^{\rm SM}_{h\to bb} \lesssim 3.2$ [75–78,89,90]. These bounds are compatible with the rates calculated taking into account the $t - t' - t''$ mixing effect on the top-quark Yukawa coupling as well as the t_2 and t_3 eigenstate contributions in the triangular loop of the gluon fusion mechanism, for our parameter sets A1/A2. This parameter set yields indeed

$$\begin{aligned} \sigma^{t'}_{gg\to h} B^{t'}_{h\to\gamma\gamma}/\sigma^{\rm SM}_{gg\to h} B^{\rm SM}_{h\to\gamma\gamma} &= 1.16(1.19); \\ \sigma^{t'}_{gg\to h} B^{t'}_{h\to WW}/\sigma^{\rm SM}_{gg\to h} B^{\rm SM}_{h\to WW} &= 1.25(1.28) \end{aligned} \tag{3}$$

$$\begin{aligned} \sigma^{t'}_{gg\to h} B^{t'}_{h\to ZZ}/\sigma^{\rm SM}_{gg\to h} B^{\rm SM}_{h\to ZZ} &= 1.25(1.28); \\ \sigma^{t'}_{gg\to h} B^{t'}_{h\to\tau\tau}/\sigma^{\rm SM}_{gg\to h} B^{\rm SM}_{h\to\tau\tau} &= 1.25(1.28) \end{aligned} \tag{4}$$

$$\sigma^{t'}_{gg\to h} B^{t'}_{h\to bb}/\sigma^{\rm SM}_{gg\to h} B^{\rm SM}_{h\to bb} = 1.25(1.28) \quad [A1]([A2]) \tag{5}$$

The cross section for the Higgs production is enhanced,

$$\sigma^{t'}_{gg\to h}/\sigma^{\rm SM}_{gg\to h} = 1.27[A1](1.31[A2]),$$

due to the combination of two possible effects: the increase of the t_1 Yukawa coupling and the constructive interferences between the t_1 contribution and the t_2, t_3 ones. In contrast, the branching fraction for the decay channel into diphoton is slightly decreased,

$$B^{t'}_{h\to\gamma\gamma}/B^{\rm SM}_{h\to\gamma\gamma} = 0.91[A1](0.90[A2]).$$

But the resulting product $\sigma^{t'}_{gg\to h}B^{t'}_{h\to\gamma\gamma}$ is increased relatively to the SM case as shown in Eq. (3). Such an increased value of the observable $\sigma_{gg\to h}B_{h\to\gamma\gamma}$, induced here by the presence of t' quarks (cf. Eq. (3)), could be indicated by the slight excess in the ATLAS [76,77,89,90] and CMS [75,78,89] data corresponding to a possible $\sim$125 GeV Higgs signal in the diphoton channel. All the values of the quantities, $\sigma^{t'}_{gg\to h}B^{t'}_{h\to\gamma\gamma}/\sigma^{\rm SM}_{gg\to h}B^{\rm SM}_{h\to\gamma\gamma}$, $\sigma^{t'}_{gg\to h}B^{t'}_{h\to WW}/\sigma^{\rm SM}_{gg\to h}B^{\rm SM}_{h\to WW}$, $\sigma^{t'}_{gg\to h}B^{t'}_{h\to ZZ}/\sigma^{\rm SM}_{gg\to h}B^{\rm SM}_{h\to ZZ}$, $\sigma^{t'}_{gg\to h}B^{t'}_{h\to\tau\tau}/\sigma^{\rm SM}_{gg\to h}B^{\rm SM}_{h\to\tau\tau}$ and $\sigma^{t'}_{gg\to h}B^{t'}_{h\to bb}/\sigma^{\rm SM}_{gg\to h}B^{\rm SM}_{h\to bb}$, in Eq. (3)–(5), are also compatible with the CMS and ATLAS best-fit values whose central value, from the combination of all search channels, is of $1.22^{+0.31}_{-0.39}$ [78] (for a Higgs mass hypothesis of 124 GeV) [91] and $0.90^{+0.40}_{-0.37}$ [90] (for a Higgs mass hypothesis of 126 GeV), respectively [93]. It is also interesting to note that the present theoretical model allows for either an increase of $\sigma^{t'}_{gg\to h}$ compared to the SM, as here for A1/A2, or a decrease as with the parameter sets in the following.

Sets B, C—For these sets of parameters where $m_h =$ 255 GeV or 320 GeV, all the Higgs decays have negligible widths relatively to the dominant channels $h\to ZZ$ and $h\to WW$, as in the SM case. Hence the branching fractions $B_{h\to ZZ}$ and $B_{h\to WW}$ remain unchanged in the present model with vectorlike top quarks where only the decay widths for $h\to t\bar{t}$, $h\to gg$, $h\to\gamma\gamma$ and $h\to\gamma Z$ are modified. In consequence, the experimental limits on $\sigma_{gg\to h}/\sigma^{\rm SM}_{gg\to h}\lesssim 0.45$ (0.40) [for $m_h\simeq 255\,(320)$ GeV] issued from the LHC combined investigations using the $h\to ZZ$, WW channels exclusively [75–78,89,90] can be applied directly to our framework where one gets

$$\sigma^{t'}_{gg\to h}/\sigma^{\rm SM}_{gg\to h} = 0.45[B];\qquad 0.40[C] \tag{6}$$

which does not conflict with the above LHC limits. Note that for the point C, $\sigma^{t'}_{gg\to h}$ is strongly reduced compared to SM. A factor 1/10 could even be achieved in the present theoretical model but variants of the multiplet choice (non-minimal in term of field content), allowing coupling correction cancellations, should then be used instead to pass the indirect constraints discussed in Sec. V.

Set D—For $m_h = 540$ GeV, the Higgs boson is searched only through its decays into ZZ and WW. The strongest bounds on the Higgs rates from the LHC read as $\sigma_{gg\to h}B_{h\to ZZ}/\sigma^{\rm SM}_{gg\to h}B^{\rm SM}_{h\to ZZ}\lesssim 0.90$ and $\sigma_{gg\to h}B_{h\to WW}/\sigma^{\rm SM}_{gg\to h}B^{\rm SM}_{h\to WW}\lesssim 1.45$ [75–78,89,90]. These upper limits are clearly in good agreement with the rates calculated in the presence of the t' and t'' states (that modifies $B_{h\to t\bar{t}}$) for the set D, namely,

$$\begin{aligned}\sigma^{t'}_{gg\to h}B^{t'}_{h\to ZZ}/\sigma^{\rm SM}_{gg\to h}B^{\rm SM}_{h\to ZZ} &= 0.69\\ \sigma^{t'}_{gg\to h}B^{t'}_{h\to WW}/\sigma^{\rm SM}_{gg\to h}B^{\rm SM}_{h\to WW} &= 0.69\end{aligned} \tag{7}$$

where

$$B^{t'}_{h\to ZZ}/B^{\rm SM}_{h\to ZZ} = 1.06 \qquad B^{t'}_{h\to WW}/B^{\rm SM}_{h\to WW} = 1.06[D].$$

V. THE INDIRECT CONSTRAINTS AND OBLIQUE PARAMETERS

Given the absence of precise measurement for the $Zt\bar{t}$ vertex (coupling directly modified by the $t-t'-t''$ mixing), the main indirect constraints to the present model come from the corrections to the gauge boson vacuum polarizations induced by the loops of $q_{5/3}$, t', t'' states. The values of the oblique parameters S, T that we obtain, according to the preliminary calculations of Ref. [94,95], are given in Table I. They appear to belong to the 1σ regions induced by the long list of EW precision observables measured mainly at the LEP collider [96]. Remark that the input parameters of Table I (i.e. the theoretical values in the first four lines) have been chosen to fix a panel of characteristic benchmark points for m_{t_2} that pass the indirect constraints as well as the bounds from direct Higgs search described in previous section; however those two types of constraints allow large domains of the parameter space (varying also m_h). The precise setting of the Y coupling reflects mainly the experimental precision on the top-quark mass measurement (and not any fine-tuning).

The t', t'' states could contribute to flavor changing neutral current reactions which are experimentally well-constrained; from the theoretical point of view, these flavor changing neutral current contributions rely precisely on the whole set of Yukawa coupling constants for the entire quark sector. The treatment of such an high degree of freedom in the parameter space is beyond the scope of the present study.

Finally, given the relative heaviness of the t_2 quark, we have checked that the predicted value for the V_{tb} CKM matrix element is in agreement with the experimental measurement close to unity obtained (without assuming 3×3 unitarity) through the single top-quark production cross section at Tevatron [96].

VI. HIGGS SIGNAL RECONSTRUCTION IN $\bar{t}_2 t_2 \to th + X$ EVENTS

We have studied the sensitivity at the LHC with $\sqrt{s} =$ 14 TeV of a search for $pp\to t_2\bar{t}_2$ production, with one of the t_2 decaying to th, and the other decaying to bW or tZ or

TABLE II. Information entering the signal event yield Y_S calculation. The t_2 pair production cross section at 14 TeV and t_2 branching fraction values are from Table I. The ratio $f^{t'/\mathrm{SM}}_{h\to VV} = B^{t'}_{h\to VV}/B^{\mathrm{SM}}_{h\to VV}$ values are calculated in Sec. IV. The event yield Y_S, per unit of integrated luminosity, is given for the different final states $\bar{t}_2 t_2 \to thbW$, $thtZ$, $thth$ and $h \to \gamma\gamma$, for points A1 and A2, or $h \to ZZ$, for points B, C, D. For $thth$ events, the event yield is calculated for the case where one h decays to vector bosons, while the second h decays inclusively. This synoptic table summarizes at once, for convenience, all the relevant numbers useful for the experimental search.

									$Y_S(h \to VV)$ (fb)		
Parameter set	m_{t_2} (GeV)	m_h (GeV)	$\sigma_{\bar{t}_2 t_2}$ (fb)	$B_{t_2\to th}$	$B_{t_2\to tZ}$	$B_{t_2\to bW}$	$B^{\mathrm{SM}}_{h\to VV}$	$f^{t'/\mathrm{SM}}_{h\to VV}$	$thbW$	$thtZ$	$thth$
Point A1	403	125	$1.353\,10^4$	0.626	0.286	0.088	$2.29\,10^{-3}$	0.91	3.11	10.1	22.1
Point A2	599	125	$1.465\,10^3$	0.821	0.147	0.032	$2.29\,10^{-3}$	0.90	0.159	0.729	4.07
Point B	626	255	$1.164\,10^3$	0.608	0.250	0.142	0.298	1.00	59.9	105	256
Point C	572	320	$1.975\,10^3$	0.135	0.461	0.404	0.309	1.00	66.6	76.0	22.2
Point D	788	540	$0.284\,10^3$	0.430	0.403	0.166	0.265	1.06	11.4	27.6	29.5

th, resulting into *thbW*, *thtZ* and *thth* final states, respectively. For a best sensitivity and in order to measure the Higgs mass precisely, we have exploited the Higgs decay channel into ZZ to four charged leptons for the signals with Higgs mass above 200 GeV (points B, C, D) while the Higgs decay into two photons is considered for the signals with a Higgs mass of 125 GeV (sets A1 and A2).

For the signal event generation, we have implemented the couplings of our t_2 model in FEYNRULES [97,98] interfaced with MADGRAPH [99] for the Monte Carlo generation, PYTHIA [100] for the hadronization part and DELPHES [101] for the fast simulation of a typical LHC detector response. Signal events are generated for the t_2 and h masses corresponding to the parameter sets described in Table I, for the three final states *thbW*, *thtZ* and *thth*. Events corresponding to points A1 and A2 are generated with the Higgs decaying through $h \to \gamma\gamma$, while for points B, C and D the $h \to ZZ$ decay is retained for the sensitivity studies described in this section. The main backgrounds were generated with ALPGEN [102] interfaced to PYTHIA and DELPHES, as for the signal events. Physics objects used for the analysis (photons, leptons and jets) were defined emulating the requirements used in real CMS Higgs searches in the 2011 data. In particular, we followed closely the physics object definition as for the real data 7 TeV Higgs analysis in the diphoton channel [103] and in the four-lepton channel [104].

In the following the quoted number of events and distributions are normalized to an integrated luminosity of 20 fb^{-1} multiplied by, for the different signal final states, their expected $\sigma_{\bar{t}_2 t_2}$ cross section times branching fractions (hereafter referred to as signal event yield per unit of integrated luminosity), while, for background processes, their ALPGEN cross sections are used. The signal event yield in the different final states depends upon the parameter set under consideration. In Table II, we summarize, for each parameter set described in Table I, the physical signal m_{t_2} and m_h masses, the $\sigma_{\bar{t}_2 t_2}$ cross sections, the t_2 branching fractions into bW ($B_{t_2\to bW}$), tZ ($B_{t_2\to tZ}$), th ($B_{t_2\to th}$) final states, as well as the h branching fractions into $\gamma\gamma$ (for sets A1 and A2) and into ZZ (for sets B, C and D), reporting the expected SM branching fraction values and the factor $f^{t'/\mathrm{SM}}_{h\to VV}$ (see Sec. IV) by which it is modified in the present model. The last three columns of Table II show the expected signal event yield, for *thbW*, *thtZ* and *thth* final states, with one Higgs boson decaying via to diphoton or ZZ final state. They are calculated as follows:

$$
\begin{aligned}
&thbW\text{final state,} && Y_S(h\to VV) = 2 && B_{t_2\to th}B_{t_2\to bW} && B^{\mathrm{SM}}_{h\to VV} f^{t'/\mathrm{SM}}_{h\to VV}\sigma_{\bar{t}_2 t_2}\\
&thtZ\text{final state,} && Y_S(h\to VV) = 2 && B_{t_2\to th}B_{t_2\to tZ} && B^{\mathrm{SM}}_{h\to VV} f^{t'/\mathrm{SM}}_{h\to VV}\sigma_{\bar{t}_2 t_2}\\
&thth\text{final state,} && Y_S(h\to VV) = 2 && B^2_{t_2\to th} && B^{\mathrm{SM}}_{h\to VV} f^{t'/\mathrm{SM}}_{h\to VV}\sigma_{\bar{t}_2 t_2}.
\end{aligned}
$$

For *thth* events, the event yield is given for events where one h decays to vector bosons, while the second h decays inclusively. The signal event yield (in fb) multiplied by the integrated luminosity (in fb^{-1}) results into the numbers of produced signal events for that luminosity. We note that, for a chosen Higgs decay, the signal yield depends on both $\sigma_{\bar{t}_2 t_2}$ and $B_{t_2\to th}$. Then, for example, in spite of the fact that $\sigma_{\bar{t}_2 t_2}$ is larger for point C than B, the signal event yield is higher for point B than C, because of the larger $B_{t_2\to th}$ value in point B. The background cross sections are listed in Table III, for the four-lepton search channel, and in Table IV for the diphoton search channel.

A. Search for $\bar{t}_2 t_2 \to th + X$ signal in the four leptons plus multijets channel

In order to estimate the sensitivity of a search for *thbW*, *thtZ* and *thth* final states, when the Higgs boson is relatively heavy, as expected for the points B, C and D, with $m_h = 255$, 320, 540 GeV, respectively, we exploit the decay channel into four charged leptons $h \to ZZ \to 4l$.

TABLE III. Cross section and number of expected events after different selection cuts (see text), for an integrated luminosity of 20 fb^{-1} at $\sqrt{s} = 14$ TeV, in the search for $thbW$, $thtZ$ and $thth$ final states, with $h \to ZZ$, in the four leptons plus multijets channel. The number of events is given separately for each signal final state ($thbW/thtZ/thth$) and for each background process. In the four rightmost columns, S, the total number of signal events (summed over all signal final states), and B, the total number of background events (summed over all background processes), are given after all selection cuts but the M_{4l} cut, in column "no M_{4l} cut", and after three different M_{4l} cut values. The S values for points B, C and D are given on the same lines as indicated in column "Parameter set". The B values in the column "no M_{4l} cut" are the sum of the individual background contributions as reported in the background column under "N_{2b}." The quantity $\Delta B = \sqrt{B}$ is the expected statistical uncertainty on the total number of background events. In the text, the signal sensitivity is given as the ratio $S/\Delta B$.

	Signal: $thbW/thtZ/thth$, $h \to ZZ$				Total signal S, M_{4l} (GeV) cut			
Parameter set	Y_S (fb)	N_{4l}	N_{N_j,H_T}	N_{2b}	no M_{4l} cut	$M_{4l} > 200$	>300	>500
Point B	59.9/105/256	8.1/23.7/37.8	5.5/18.0/28.9	3.52/11.5/18.5	33.4	30.4	17.0	4.9
Point C	66.6/76.0/22.2	7.7/15.8/3.1	4.8/11.3/2.2	3.07/7.23/1.41	11.7	10.7	7.4	2.0
Point D	11.4/27.6/29.5	1.5/6.6/4.7	1.1/5.3/3.9	0.70/3.40/2.50	6.6	6.2	5.1	2.7
		Background			Total background B, M_{4l} (GeV) cut			
Process	σ (fb)	N_{4l}	N_{N_j,H_T}	N_{2b}	no M_{4l} cut	$M_{4l} > 200$	>300	>500
$t\bar{t}$ + jets	$9.19\,10^5$	4680	1480	27.5	35.5	23.5	13.2	6.8
$t\bar{t}b\bar{b}$ + jets	$2.50\,10^3$	5.60	3.10	2.0	Statistical ΔB, M_{4l} (GeV) cut			
$t\bar{t}W$ + jets	$1.99\,10^2$	1.20	0.40	0.036	no M_{4l} cut	$M_{4l} > 200$	>300	>500
$t\bar{t}Z$ + jets	97.3	25.0	9.5	6.0	6.0	4.9	3.6	2.6

Signals from $thbW$, $thtZ$, $thth$, $h \to ZZ \to 4l$, final states are characterized by four high transverse momentum leptons, from the Higgs decay, and a large number of energetic jets, from accompanying top and heavy vector boson decays.

The event selection, exploiting the large number of high transverse momentum (p_T) leptons and jets, as well as the b-jet content of the event, consists of the following criteria:

(i) Four leptons (muons or electrons) are required with transverse momentum $p_T > 20$ GeV and pseudorapidity $|\eta| < 2.4$ or 2.5 for muons or electrons, respectively, and two lepton pairs, each pair with same flavor but opposite charge leptons. The lepton pair of highest p_T is required to have a dilepton invariant mass consistent with the Z mass, $M_{2l} = M_Z \pm 15$ GeV, while the lepton pair with second highest dilepton p_T must have a dilepton invariant mass $M_{2l} > 12$ GeV;

(ii) $H_T > 1000$ GeV and $N_j > 5$, with H_T being defined as the scalar sum of the transverse momenta of identified leptons, photons, jets, and the missing energy, and N_j being the number of hadronic jets with $p_T > 30$ GeV and $|\eta| < 2.4$;

(iii) At least two b-tagged jets in the event.

TABLE IV. Cross section and number of expected events after different selection cuts (see text), for an integrated luminosity of 20 fb^{-1} at $\sqrt{s} = 14$ TeV, in the search for $thbW$, $thtZ$ and $thth$ final states, with $h \to \gamma\gamma$, in the diphoton plus multijets channel. The number of events is given separately for each signal final state ($thbW/thtZ/thth$) and for each background process. In the two rightmost columns, S, the total number of signal events (summed over all signal final states), and B, the total number of background events (summed over all background processes), are given after all selection cuts in column "$M_{2\gamma} > 90$" and within a mass window $M_{2\gamma} \in [115, 135]$ GeV in the next column. The S values for points A1 and A2 are given in the same lines as indicated in column "Parameter set". The B values in the column "$M_{2\gamma} > 90$" are the sum of the individual background contributions as reported in the background column under "$N_{N_j>8}$". The quantity $\Delta B = \sqrt{B}$ is the expected statistical uncertainty on the total number of background events. In the text, the signal sensitivity is given as the ratio $S/\Delta B$.

	Signal: $thbW/thtZ/thth$, $h \to \gamma\gamma$				Total signal S, $M_{2\gamma}$ (GeV) cut	
Parameter set	Y_S (fb)	$N_{2\gamma}$	$N_{N_j>6}$	$N_{N_j>8}$	$M_{2\gamma} > 90$	$M_{2\gamma} \in [115, 135]$
Point A1	3.1/10.1/22.1	5.4/15.4/30.4	4.1/12.7/27.1	1.4/6.2/14.5	22.1	17.7
Point A2	0.16/0.73/4.1	0.34/1.35/6.98	0.27/1.17/6.6	0.10/0.62/3.8	4.5	3.2
		Background			Total background B, $M_{2\gamma}$ (GeV) cut	
Process	σ (fb)	$N_{M_{2\gamma}>90}$	$N_{N_j>6}$	$N_{N_j>8}$	$M_{2\gamma} > 90$	$M_{2\gamma} \in [115, 135]$
$W\gamma\gamma$ + jets	450	422	110	19.6	27.8	4.38
$t\bar{t}\gamma\gamma$ + jets	15.5	11.8	11.3	8.18	Statistical ΔB, $M_{2\gamma}$ (GeV) cut	
$t\bar{t}W\gamma\gamma$ + jets	0.0678	0.0577	0.0515	0.0272	$M_{2\gamma} > 90$	$M_{2\gamma} \in [115, 135]$
					5.3	2.1

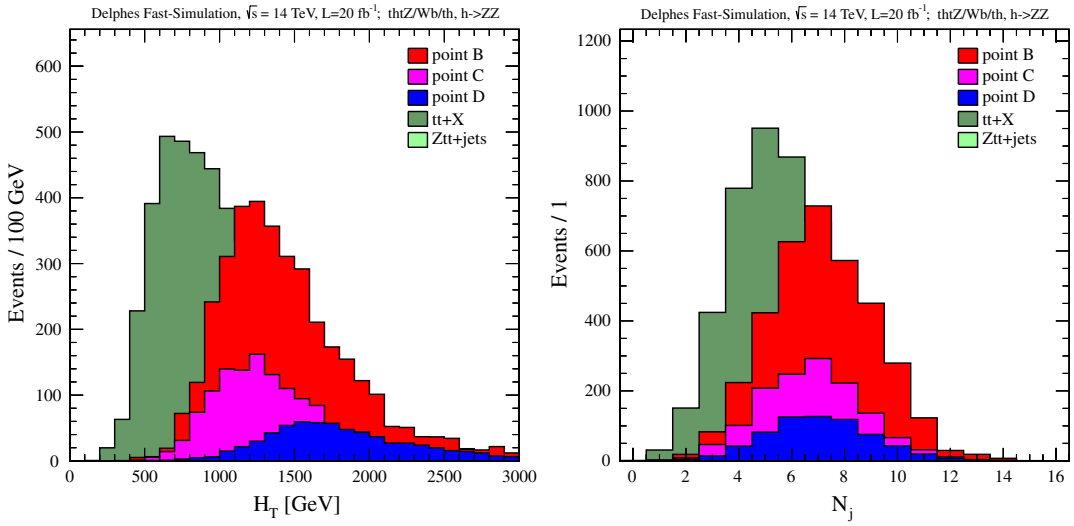

FIG. 1 (color online). Distributions of the H_T variable and the jet multiplicity N_j after four-lepton requirements. Background and signal distributions are shown overlaid, to compare the different distribution shapes, with the background normalized to the expected events for 20 fb^{-1} and the corresponding signal expectation multiplied by a factor of 50.

The motivation for the H_T and N_j cuts is evident from Fig. 1, showing the H_T and N_j distributions after the four-lepton requirements. The event numbers are shown for an integrated luminosity $L = 20$ fb^{-1}, with the signal event numbers multiplied by a factor of 50, for shape comparison. Expectations for the signals, by final state, and the backgrounds processes, after the selection cuts, for an integrated luminosity of $L = 20$ fb^{-1}, are shown in Table III, where the following quantities are reported:

(i) Y_S, the signal event number produced, per unit of integrated luminosity, given for each signal parameter set and final state under study, as reported in Table II;

(ii) σ, the cross sections, as calculated by the ALPGEN generator, for the background processes included in the present study;

(iii) N_{4l}, the number of events after four-lepton requirements;

(iv) N_{N_j,H_T}, the number of events after the additional requirements $H_T > 1000$ GeV and $N_j > 5$;

(v) N_{2b}, the number of events after the additional requirements of two b-tagged jets in the event;

(vi) S and B, the total number of signal (summed over all signal final states) and background (summed over all background processes), after a cut on the reconstructed four-lepton invariant mass, M_{4l}, with ΔB being the expected uncertainty on the total number of background events. Here we only consider the statistical uncertainty $\Delta B = \sqrt{B}$, but a more realistic estimation should also include systematic uncertainties on the number of background events. Some of the dominant systematic uncertainties are depending on detector effects (for instance jet energy resolution) and can be best evaluated with real data. In the following, an estimation of the signal sensitivity is given as the ratio $S/\Delta B$, measuring the signal in terms of background standard deviations.

The need for additional cuts, after the leptons, jets and H_T requirements, is seen in Table III, where the N_{N_j,H_T} column shows that after these cuts, a large background, predominantly from $t\bar{t}$ + jets production, is still present. Further background rejection can be obtained with requirements on the number of b-tagged jets. The motivation is the following: in $t\bar{t}$ events the requirement of four high p_T leptons strongly reduces the number of b-taggable jets. Indeed, in $t\bar{t}$ + jets events, while two high p_T leptons are provided by the two leptonic W decay, the additional two leptons are preferentially resulting from the two b decays. Thus, applying a b-tagging requirement can reduce significantly the $t\bar{t}$ contribution. In the signal case, the four leptons come mainly from the $h \to ZZ \to 4l$ decay so that there are in average at least two b-taggable jets in the event, for which a b-tagging requirement can have high efficiency. Since no detailed b-tagging information is presently available in DELPHES, we make use of known b-tagging and mistagging efficiency values as measured by LHC experiments (see e.g. Ref. [105]), to estimate the effect on background and signal of requiring two b-tagged jets in the event. The probability for a b-jet to be b-tagged is taken to be $\epsilon_{b\text{-tag}} = 0.8$ and for a mistagging the probability is $\epsilon_{\text{mis-tag}} = 0.05$. An event-by-event weight, that is an estimation of the probability that two b-jets be identified in the event, is applied to both background and signal events. The number of expected events, for signals and backgrounds, resulting from leptons, jets and b-tagging requirement are shown in the column N_{2b} of Table III.

The corresponding distributions of the invariant mass of the four leptons, M_{4l}, for signals and backgrounds are shown in Fig. 2. The mass peak corresponding to the generated Higgs mass is reconstructed at the correct mass value with good resolution ($\Delta M_{4l}/M_{4l} \lesssim 10\%$). Signal events, with reconstructed mass significantly lower, or higher, than the generated Higgs mass value, are in general events where one lepton from the $h \to ZZ \to 4l$ decay does not pass the lepton selection criteria, while another lepton from an accompanying W or Z decays is selected to reconstruct the four-lepton invariant mass. The background, mainly from the $t\bar{t}$ + jets process, is mostly concentrated in the M_{4l} region below 200 GeV. Applying a lower cut on M_{4l} removes a large fraction of the background and improves the signal significance, as shown in Table III.

An additional distribution of the variable, M_{4l3j}, is shown after all but the M_{4l} cuts. This variable can help estimating directly the mass of the heavy toplike quark. It is defined as the invariant mass of the system obtained by associating to the four-lepton momentum direction the three closest jets (expected to come from the decay of the accompanying top quark, $t \to bW$, $W \to 2$ jets), choosing among all the jets in the event those with the smallest $\Delta R \equiv \sqrt{\Delta\eta^2 + \Delta\phi^2}$ with respect to the four-lepton momentum direction. The distributions of M_{4l3j} for signals and backgrounds are shown in Fig. 2. A broad peak, whose width is dominated by the jet energy resolution and jet combinatorics, is observed centered at about the generated t_2 mass value (the t_2 physical width is given in Table I) for the points B and C having larger t_2 pair production rates than for the set D. Therefore, this mass reconstruction method, together with the four-lepton mass reconstruction, will give an early indication that a heavy particle has been produced in the collision and decayed into a Higgs boson (identified by the four-lepton mass peak) plus three jets. Another mass reconstruction method, described in the next section, that exploits the property of the two heavy particles having equal mass, will give another characterization of the origin of the observed signal. Ultimately, a kinematic fit technique (utilized, for instance, in top-quark mass measurements, see e.g. [106]), to test on an event-by-event basis the hypothesis that the event results from the production of two heavy particles of equal mass (see e.g. [107])—one of which decays into two particles with known decays and masses (three jets, with invariant mass around the top mass, and four leptons, with invariant mass around the value measured from the four-lepton mass peak, see Fig. 2)—can be properly applied in real data events, when the detailed parametrizations of the experimental resolutions of the physics objects entering the fit can be obtained from data.

The numbers of signal and background events expected after all cuts, and for $M_{4l} > 200$, 300 and 500 GeV, are shown in the three rightmost columns of Table III together with the expected statistical background standard deviation ΔB for the three signal points investigated in this search channel. We estimate that, for an integrated luminosity of 20 fb^{-1}, a signal corresponding to point B is detectable with a significance $S/\Delta B \sim 6$ (after $M_{4l} > 200$ GeV cut). For this benchmark point the $B_{t_2 \to th}$ branching fraction is $\sim$0.6. Then, for similar t_2 cross section, t_2 mass and h mass values, a signal could be discovered, with $S/\Delta B \gtrsim 5$, for $B_{t_2 \to th} \gtrsim 0.5$. For point C, with $B_{t_2 \to th} \sim 0.1$ we obtain a signal significance $S/\Delta B \sim 2$. A signal significance of five and above is then obtained for $B_{t_2 \to th} \gtrsim 0.25$. For smaller

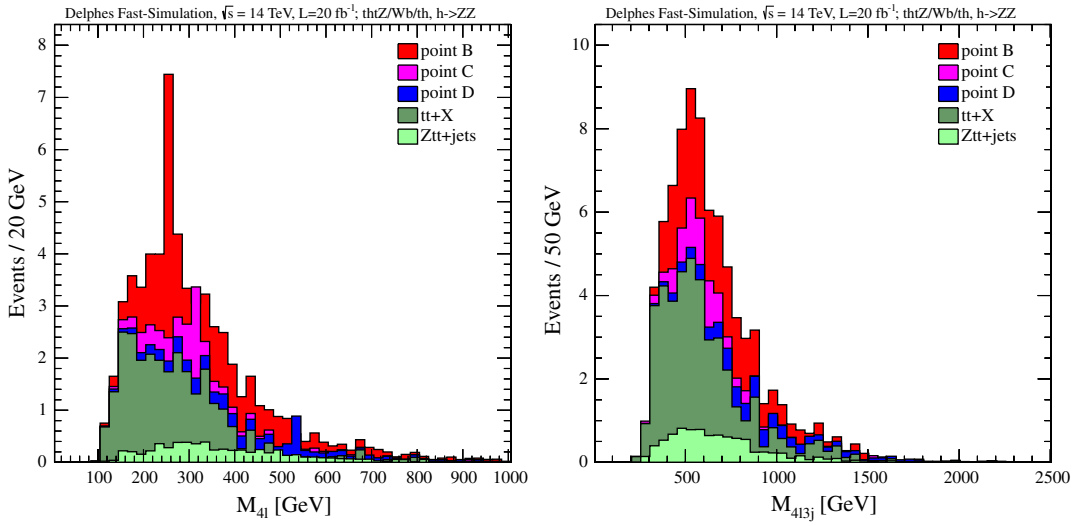

FIG. 2 (color online). Distributions of the four-lepton invariant mass, M_{4l}, and of the reconstructed heavy top-partner mass, M_{4l3j} (see text), after all selection cuts. Signal and background distributions, normalized to the expected events for 20 fb^{-1}, are shown stacked to indicate their relative contributions. Signal distributions for points B, C and D correspond to Higgs mass $m_h = 255$, 320 and 540 GeV, respectively.

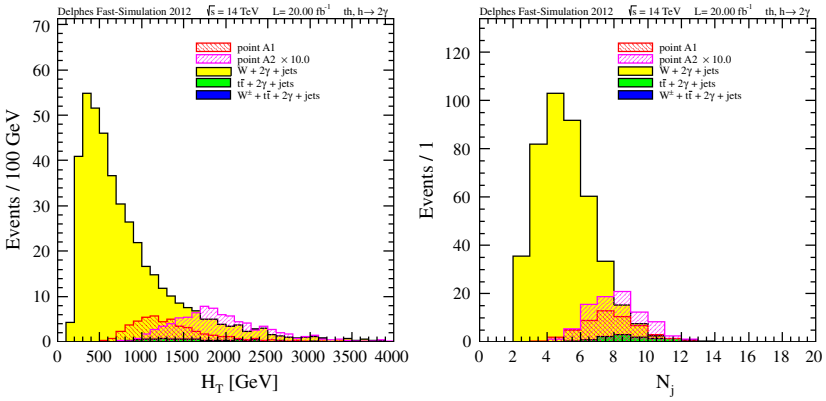

FIG. 3 (color online). Distributions of the H_T variable and the jet multiplicity N_j after diphoton requirements, including a diphoton invariant mass cut $M_{2\gamma} > 90$ GeV.

$B_{t_2 \to th}$ values, a larger integrated luminosity, or a more optimal analysis, would be needed for a signal significance of five or above. For point D, with $B_{t_2 \to th} \sim 0.4$, we obtain a signal significance $S/\Delta B \sim 1.4$ thus even for maximal $B_{t_2 \to th} \sim 1$ a signal significance of $\sim$3.5 is attainable. Higher integrated luminosity, or higher background rejection, depending on the $B_{t_2 \to th}$ value (for $B_{t_2 \to th} \sim 0.4$, about a factor of 10 larger luminosity or background rejection) is needed for a five-sigma signal significance corresponding to the D scenario, with a t_2 mass of about 800 GeV and a pair production cross section of about 0.3 pb.

B. Search for $\bar{t}_2 t_2 \to th + X$ signal in the diphoton plus multijets channel

To study the sensitivity of a search for $thtZ$, $thbW$ and $thth$ final states, when the Higgs boson is relatively light, as for points A1 and A2, with $m_h = 125$ GeV, we exploit the $h \to \gamma\gamma$ decay channel. As for a light Higgs boson in the SM, in spite of the relatively small expected $B(h \to \gamma\gamma)$ value, this is expected to be a channel with good signal sensitivity, due to the good diphoton mass resolution, allowing to identify the Higgs mass signal over a background that can be well-measured in the sidebands.

The background processes considered in this study are listed in Table IV. To reduce generation time for the background events, we have applied cuts on ALPGEN-generated parton quantities, that are looser than the cuts applied on the reconstructed physics objects. The generator-level cuts are: photon $p_T > 20$ GeV and $|\eta| < 3.0$, jet $p_T > 20$ GeV and $|\eta| < 2.5$, $\Delta R_{\gamma j} < 0.4$, $\Delta R_{\gamma l} < 0.4$, $\Delta R_{jj} < 0.4$ and $\Delta R_{t\bar{t}} < 0.4$. Background cross sections for these generator-level cuts as calculated by ALPGEN are listed in Table IV. An additional background is the $\gamma\gamma$ + jets process. A relatively large inclusive diphoton cross section is expected [108] and is going to be measured at the LHC, together with the contribution from fake diphoton pairs. The inclusive diphoton cross section in the diphoton mass region of interest can be large (order of pb), but we expect that the large jet multiplicity requirement scales down this contribution by at least 3 orders of magnitude, thus reducing its cross section to few fb. An additional handle to minimize this background will be the b-tagging, that can reduce the contribution from light flavored multijets events by 2 or 3 order of magnitudes (as discussed in the previous section), while retaining a large fraction of the signal events containing at least two b-jets. However, b-tagging will not effectively reduce backgrounds with t-quark pairs in the final state, as in the case of $t\bar{t}\gamma\gamma$ + jets process. Thus, conservatively we have not exploited b-tagging for this analysis of the $h \to \gamma\gamma$ channel.

Signals from $thbW$, $thtZ$, $thth$, $h \to \gamma\gamma$, final states are characterized by a large number of energetic jets, from top and heavy vector boson decays, in addition to the two high-transverse-momentum photons from the Higgs decay. The event selection consists of the following criteria:

(i) Photons are required to be within $|\eta| < 2.5$ and isolated. The isolation requirements imply that, within a cone $\Delta R = 0.4$ around the photon direction, the charged particle energy measured in the tracker is <2.0 GeV, the electromagnetic calorimeter (ecal) energy in the cone is <4.2 GeV, the hadronic calorimeter (hcal) energy in the cone is <2.2 GeV and the ratio between the ecal and hcal energy in the cone is <0.05. Two isolated photons are required, with the leading photon $p_T > 45$ GeV and the second photon $p_T > 30$ GeV. The invariant mass of the two photons is required to be $M_{2\gamma} > 90$ GeV.

(ii) Hadronic jets are counted if they have $p_T > 30$ GeV and $|\eta| < 2.4$. Events are required to have a number of jets $N_j > 6$, at preselection, or $N_j > 8$, for the final selection, after which the signal sensitivity is evaluated in a sliding window in the diphoton invariant mass $M_{2\gamma}$.

Figure 3 shows the H_T and N_j distributions after the after diphoton requirements, including a diphoton invariant

mass cut $M_{2\gamma} > 90$ GeV. The distributions are shown for an integrated luminosity $L = 20$ fb^{-1}, with the signal expectation for point A2 multiplied by a factor of 10, for shape comparison. Because of the relatively light t_2 mass in point A1, an $H_T > 1000$ GeV cut, as applied for points B, C and D, would reject a significant fraction of this signal. A lower H_T cut would not improve significantly the signal-over-background ratio after the N_j requirement, thus no H_T cut is applied in this channel. Expectations for the signals, by final state, and the backgrounds processes, after the selection cuts, for an integrated luminosity of $L = 20$ fb^{-1}, are shown in Table IV, where the following quantities are reported:

(i) Y_S, the signal event number produced, per unit of integrated luminosity, given for each signal parameter set and final state under study, as reported in Table II;

(ii) σ, the background cross sections, as calculated from the ALPGEN generator, for the background processes included in the present study;

(iii) $N_{2\gamma}$, the number of events after diphoton and $M_{2\gamma} > 90$ GeV requirements;

(iv) $N_{N_j>6}$ and $N_{N_j>8}$ the number of events after the additional jet multiplicity cuts;

(v) S and B, the total number of signal (summed over all signal final states) and background (summed over all background processes), after a cut $M_{2\gamma}$, with ΔB being the expected statistical uncertainty (standard deviation) on the total number of background events. An estimation of the expected signal sensitivity can then be evaluated as the ratio $S/\Delta B$, measuring the signal in terms of background standard deviations.

In virtue of the good diphoton mass resolution ($\sim 1\%$ to 5% for a 110 to 130 GeV Higgs boson, depending on photon selection criteria) of the detector, a highly discriminating quantity after selection is the reconstructed diphoton mass. The diphoton invariant mass distribution for signals and backgrounds events, after the $N_j > 8$ requirement, is shown in Fig. 4. Also shown is the distribution of an additional variable, $M_{re\,nj}$, that could help estimating the mass of the heavy toplike quark. This is defined as the invariant mass of the system of n jets recoiling against the diphoton + m jets system, where the m jets are the closest in ΔR to the diphoton direction. The recoiling n jets, with $n = N_j - m$, are counted to minimize, among all m and n choices in the event, the difference between the mass of the diphoton + m jets system and the mass of the recoiling n jets. The goal of this procedure is to separate the event into two hemispheres, one identified by the diphoton + m jets system and the other by the recoiling n jets, with m and n chosen in such a way that the invariant masses of the physics objects in the two hemispheres are about the same (within resolution), as in the case of two heavy particles decaying in diphoton plus jets, in one hemisphere, and into jets, in the other hemisphere. On the distributions of $M_{re\,nj}$ for signals and backgrounds, after all but the $M_{2\gamma}$ window cut, shown in Fig. 4, a broad peak, whose width is dominated by the jet energy resolution, is observed centered at about the generated t_2 masses. Hence, this mass reconstruction method will provide an early indication that two heavy particles of equal mass have been produced in the event and a first estimation of the t_2 mass. In real data, where the detailed measurements of the experimental resolutions are available, kinematic fits can be applied to test the pair production and decay hypothesis and possibly to reduce the uncertainty on the t_2 mass estimation.

The total number of signal and background events, after diphoton and jet multiplicity requirements, with a diphoton mass in the window between 115 GeV and 135 GeV, is also given in Table IV. We estimate that for an integrated luminosity of 20 fb^{-1}, a signal, corresponding to the benchmark point A1, is detectable with a significance

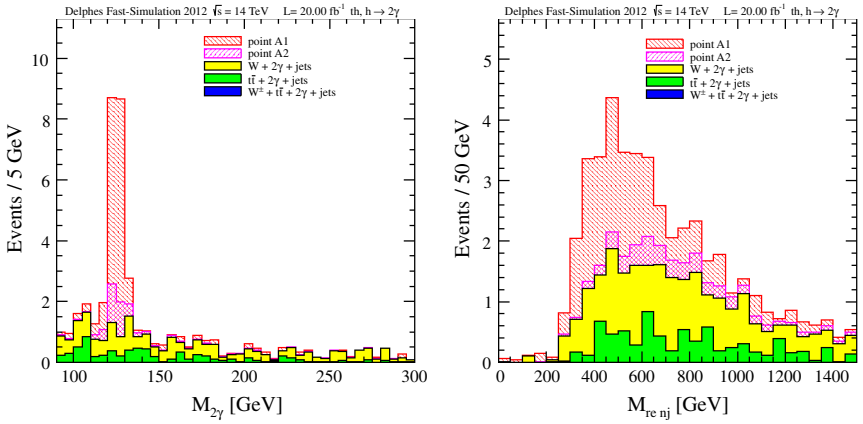

FIG. 4 (color online). Distributions of the diphoton mass, $M_{2\gamma}$, and of the reconstructed heavy recoil mass, $M_{re\,nj}$ (see text), after all selection cuts. Signal and background distributions, normalized to the expected events for 20 fb^{-1}, are shown stacked to indicate their relative contributions. Signal distributions for points A1 and A2 correspond to a Higgs mass $m_h = 125$ GeV.

$S/\Delta B \sim 9$. For this benchmark point the $B_{t_2 \to th} \sim 0.6$. Then, for a similar t_2 cross section and t_2, h mass values, a signal could still be discovered, with a signal significance of about or above five, if $B_{t_2 \to th} \gtrsim 0.3$. For point A2, where the $\sigma_{\bar{t}_2 t_2}$ is about an order of magnitude lower than in point A1, while $B_{t_2 \to th} \sim 0.8$, the expected signal significance is $\sim$1.5. Then, to reach a signal significance of five, at least a factor of 10 larger luminosity, or a better background rejection, is needed to observe this signal.

VII. CONCLUSIONS

In this paper, we have shown that there exist regions of the parameter space in beyond SM scenarios, allowed by present phenomenological and experimental constraints, in particular, by the direct Higgs searches, where heavy vectorlike top partner production at the LHC may give rise to new Higgs production channels, over a large Higgs mass range, extending from $\sim$120 GeV to more than 500 GeV. Indeed the SM Higgs mass exclusion, in the range between $\sim$130 and 600 GeV, does not hold in these beyond SM scenarios. In this context, we have also illustrated how the possible observation of a 125 GeV Higgs signal in the diphoton channel at LHC, with a cross section larger than expected in the SM, could be compatible with the presence of vectorlike heavy quarks.

We have shown that for a variety of characteristic top partner and Higgs mass values, the expected heavy top pair production cross sections and decay branching fractions lead to a signal of Higgs production (from the decay of the heavy top quark) which could be detectable at the 14 TeV LHC, with an integrated luminosity between $\sim$20 fb^{-1} and $\sim$200 fb^{-1}, over a large Higgs mass range ($\sim$ 120 GeV to $\sim$550 GeV). The good diphoton and four-lepton invariant mass resolution ($\lesssim 10\%$), in spite of the large number of jets present in the signal events, makes the discovery possible with moderate luminosity. Finally, we have proposed new mass variables from which the heavy top mass could be estimated.

ACKNOWLEDGMENTS

The work of G. M. is supported by the Institut Universitaire de France as well as the ANR CPV-LFV-LHC under Project No. NT09-508531 and TAPDMS under Project No. 09-JCJC-0146. D. K. G. acknowledges partial support from the Department of Science and Technology, India under the Grant No. SR/S2/HEP-12/2006.

[1] N. Arkani-Hamed, A. G. Cohen, and H. Georgi, Phys. Lett. B **513**, 232 (2001).
[2] N. Arkani-Hamed, A. Cohen, E. Katz, A. Nelson, T. Gregoire, and J. Wacker, J. High Energy Phys. 08 (2002) 021.
[3] N. Arkani-Hamed, A. Cohen, E. Katz, and A. Nelson, J. High Energy Phys. 07 (2002) 034.
[4] R. Contino, Y. Nomura, and A. Pomarol, Nucl. Phys. **B671**, 148 (2003).
[5] K. Agashe, R. Contino, and A. Pomarol, Nucl. Phys. **B719**, 165 (2005).
[6] K. Agashe and R. Contino, Nucl. Phys. **B742**, 59 (2006).
[7] R. Contino, L. Da Rold, and A. Pomarol, Phys. Rev. D **75**, 055014 (2007).
[8] G. Burdman and L. Da Rold, J. High Energy Phys. 12 (2007) 086.
[9] C. T. Hill, Phys. Lett. B **266**, 419 (1991).
[10] H.-C. Cheng, B. A. Dobrescu, and C. T. Hill, Nucl. Phys. **B589**, 249 (2000).
[11] M. S. Carena, E. Ponton, J. Santiago, and C. E. M. Wagner, Nucl. Phys. **B759**, 202 (2006).
[12] M. S. Carena, E. Ponton, J. Santiago, and C. E. M. Wagner, Phys. Rev. D **76**, 035006 (2007).
[13] L. Randall and R. Sundrum, Phys. Rev. Lett. **83**, 3370 (1999).
[14] M. Gogberashvili, Int. J. Mod. Phys. D **11**, 1635 (2002).
[15] T. Gherghetta and A. Pomarol, Nucl. Phys. **B586**, 141 (2000).
[16] K. Agashe, A. Delgado, M. J. May, and R. Sundrum, J. High Energy Phys. 08 (2003) 050.
[17] C. Bouchart and G. Moreau, Nucl. Phys. **B810**, 66 (2009).
[18] A. Djouadi, G. Moreau, and F. Richard, Nucl. Phys. **B773**, 43 (2007).
[19] A. Djouadi, G. Moreau, and R. K. Singh, Nucl. Phys. **B797**, 1 (2008).
[20] K. Agashe, R. Contino, L. Da Rold, and A. Pomarol, Phys. Lett. B **641**, 62 (2006).
[21] C. Bouchart and G. Moreau, Phys. Rev. D **80**, 095022 (2009).
[22] C. Kilic, K. Kopp, and T. Okui, Phys. Rev. D **83**, 015006 (2011).
[23] S. J. Huber and Q. Shafi, Phys. Lett. B **498**, 256 (2001).
[24] S. J. Huber and Q. Shafi, Phys. Lett. B **512**, 365 (2001).
[25] S. J. Huber and Q. Shafi, Phys. Lett. B **544**, 295 (2002).
[26] S. J. Huber and Q. Shafi, Phys. Lett. B **583**, 293 (2004).
[27] S. Chang, C. Kim, and M. Yamaguchi, Phys. Rev. D **73**, 033002 (2006).
[28] G. Moreau and J. Silva-Marcos, J. High Energy Phys. 03 (2006) 090.
[29] G. Moreau and J. Silva-Marcos, J. High Energy Phys. 01 (2006) 048.
[30] K. Agashe, G. Perez, and A. Soni, Phys. Rev. D **71**, 016002 (2005).
[31] K. Agashe, G. Perez, and A. Soni, Phys. Rev. Lett. **93**, 201804 (2004).
[32] K. Agashe, G. Perez, and A. Soni, Phys. Rev. D **75**, 015002 (2007).

[33] K. Agashe, A. E. Blechman, and F. Petriello, Phys. Rev. D **74**, 053011 (2006).

[34] Y. Grossman and M. Neubert, Phys. Lett. B **474**, 361 (2000).

[35] T. Appelquist, B. A. Dobrescu, E. Ponton, and H.-U. Yee, Phys. Rev. D **65**, 105019 (2002).

[36] T. Gherghetta, Phys. Rev. Lett. **92**, 161601 (2004).

[37] G. Moreau, Eur. Phys. J. C **40**, 539 (2005).

[38] F. del Aguila, J. Aguilar-Saavedra, B. Allanach, J. Alwall, Y. Andreev *et al.*, Eur. Phys. J. C **57**, 183 (2008).

[39] M. Raidal, A. van der Schaaf, I. Bigi, M. Mangano, Y. K. Semertzidis *et al.*, Eur. Phys. J. C **57**, 13 (2008).

[40] G. Cacciapaglia, A. Deandrea, D. Harada, and Y. Okada, J. High Energy Phys. 11 (2010) 159.

[41] G. Cacciapaglia, A. Deandrea, L. Panizzi, N. Gaur, D. Harada *et al.*, arXiv:1108.6329.

[42] S. Gopalakrishna, T. Mandal, S. Mitra, and R. Tibrewala, Phys. Rev. D **84**, 055001 (2011).

[43] J. Aguilar-Saavedra, Phys. Lett. B **625**, 234 (2005).

[44] J. Aguilar-Saavedra, J. High Energy Phys. 11 (2009) 030.

[45] A. Ivanov (CDF and D0 Collaboration), arXiv:1109.1025.

[46] G. Burdman, M. Perelstein, and A. Pierce, Phys. Rev. Lett. **90**, 241802 (2003).

[47] T. Han, H. E. Logan, B. McElrath, and L.-T. Wang, Phys. Rev. D **67**, 095004 (2003).

[48] M. Perelstein, M. E. Peskin, and A. Pierce, Phys. Rev. D **69**, 075002 (2004).

[49] H.-C. Cheng, I. Low, and L.-T. Wang, Phys. Rev. D **74**, 055001 (2006).

[50] G. Cacciapaglia, S. Choudhury, A. Deandrea, N. Gaur, and M. Klasen, J. High Energy Phys. 03 (2010) 059.

[51] N. Vignaroli, Nuovo Cimento Soc. Ital. Fis. C **34**, 6 (2011).

[52] R. Contino and G. Servant, J. High Energy Phys. 06 (2008) 026.

[53] C. Dennis, M. Karagoz, G. Servant, and J. Tseng, arXiv: hep-ph/0701158.

[54] K. Agashe and G. Servant, J. Cosmol. Astropart. Phys. 02 (2005) 002.

[55] G. Brooijmans *et al.* (New Physics Working Group), arXiv:1005.1229.

[56] C. Bini, R. Contino, and N. Vignaroli, J. High Energy Phys. 01 (2012) 157.

[57] R. Barcelo, A. Carmona, M. Masip, and J. Santiago, Phys. Lett. B **707**, 88 (2012).

[58] R. Barcelo, A. Carmona, M. Chala, M. Masip, and J. Santiago, Nucl. Phys. **B857**, 172 (2012).

[59] F. del Aguila, L. Ametller, G. L. Kane, and J. Vidal, Nucl. Phys. **B334**, 1 (1990).

[60] F. del Aguila, G. L. Kane, and M. Quiros, Phys. Rev. Lett. **63**, 942 (1989).

[61] G. D. Kribs, A. Martin, and T. S. Roy, Phys. Rev. D **84**, 095024 (2011).

[62] The single production becomes dominant typically around $m_{t'} \sim 700$ GeV as in the scenario with a singlet t' [43] or in little Higgs models [63].

[63] G. Azuelos, K. Benslama, D. Costanzo, G. Couture, J. Garcia *et al.*, Eur. Phys. J. C **39**, 13 (2004).

[64] Note that adding the contribution of the t' single production would increase the Higgs production rate.

[65] A. Djouadi and G. Moreau, Phys. Lett. B **660**, 67 (2008).

[66] A. Djouadi, G. Moreau, F. Richard, and R. K. Singh, Phys. Rev. D **82**, 071702 (2010).

[67] A. Djouadi, G. Moreau, and F. Richard, Phys. Lett. B **701**, 458 (2011).

[68] A. Azatov, M. Toharia, and L. Zhu, Phys. Rev. D **82**, 056004 (2010).

[69] t' representations (to which SM fields are promoted) with analog rate suppression effects can arise with the O(3) subgroup [20] implementable in the composite Higgs model [70,71] and RS scenario [72,73] which can reach strong suppressions, respectively, of $\sigma_{gg\to h}/\sigma^{\mathrm{SM}}_{gg\to h} \sim 35\%$ and $\sim 10\%$.

[70] A. Falkowski, Phys. Rev. D **77**, 055018 (2008).

[71] J. Espinosa, C. Grojean, and M. Muhlleitner, J. High Energy Phys. 05 (2010) 065.

[72] F. Ledroit, G. Moreau, and J. Morel, J. High Energy Phys. 09 (2007) 071.

[73] S. Casagrande, F. Goertz, U. Haisch, M. Neubert, and T. Pfoh, J. High Energy Phys. 09 (2010) 014.

[74] A. Djouadi, Phys. Lett. B **435**, 101 (1998).

[75] CMS web p., https://twiki.cern.ch/twiki/bin/view/CMSPublic/PhysicsResults, 2012.

[76] ATLAS web p., https://twiki.cern.ch/twiki/bin/view/AtlasPublic, 2012.

[77] ATLAS Collaboration, Phys. Lett. B **710**, 49 (2012).

[78] S. Chatrchyan *et al.* (CMS Collaboration), Phys. Lett. B **710**, 26 (2012).

[79] Such a heavy Higgs would be neither SM-like, as disfavored by the EW precision tests, nor belonging to a supersymmetric extension, as forbidden by the Higgs sector structure. However, it could perfectly be e.g. in a RS scenario where its contributions to the oblique T parameter can be compensated by new KK-induced contributions.

[80] The top quark exchange in the loop is the dominant contribution in the SM.

[81] Similar results are expected in such a situation.

[82] Namely the last two lines and columns of this mass matrix.

[83] S. Chatrchyan *et al.* (CMS Collaboration), arXiv:1203.5410 [Phys. Lett. B (to be published)].

[84] S. Chatrchyan *et al.* (CMS Collaboration), Phys. Rev. Lett. **107**, 271802 (2011).

[85] M. Aliev, H. Lacker, U. Langenfeld, S. Moch, P. Uwer, and M. Wiedermann, Comput. Phys. Commun. **182**, 1034 (2011).

[86] S. Dittmaier *et al.* (LHC Higgs Cross Section Working Group), arXiv:1101.0593, https://twiki.cern.ch/twiki/bin/view/LHCPhysics/CrossSections.

[87] G. Aad *et al.* (ATLAS Collaboration), arXiv:1202.3076 [Phys. Rev. Lett. (to be published)].

[88] We have also checked that the Tevatron constraints are satised.

[89] CERN Council Presentation, December 2011: http://indico.cern.ch/conferenceDisplay.py?confId=164890, 2011.

[90] ATLAS Collaboration, Report No. ATLAS-CONF-2012-019, 2012.

[91] This number has just been updated to $0.94^{+0.26}_{-0.34}$ for a 125 GeV Higgs [92].

[92] M. Pieri (CMS Collaboration), in Searches for the SM Scalar Boson at CMS, Recontres de Moriond EW 2012, Moriond, France, March 3-10, 2012 (unpublished).

[93] The present parameters lead to a Higgs rate, for the WW channel, standing slightly outside the 1σ range but the experimental error bars obtained by both the ATLAS and CMS Collaborations are signicant.
[94] R. Barbieri, L. J. Hall, Y. Nomura, and V. S. Rychkov, Phys. Rev. D **75**, 035007 (2007).
[95] L. Lavoura and J. P. Silva, Phys. Rev. D **47**, 2046 (1993).
[96] K. Nakamura *et al.* (Particle Data Group), J. Phys. G **37**, 075021 (2010).
[97] N. D. Christensen and C. Duhr, Comput. Phys. Commun. **180**, 1614 (2009).
[98] We thank Claude Duhr and Benjamin Fuks for their precious help in this implementation.
[99] M. Herquet and F. Maltoni, Nucl. Phys. B, Proc. Suppl. **179–180**, 211 (2008).
[100] T. Sjostrand, S. Mrenna, and P. Z. Skands, J. High Energy Phys. 05 (2006) 026.
[101] S. Ovyn, X. Rouby, and V. Lemaitre, arXiv:0903.2225.
[102] M. L. Mangano, M. Moretti, F. Piccinini, R. Pittau, and A. D. Polosa, J. High Energy Phys. 07 (2003) 001.
[103] S. Chatrchyan *et al.* (CMS Collaboration), Phys. Lett. B **710**, 403 (2012).
[104] S. Chatrchyan *et al.* (CMS Collaboration), Phys. Rev. Lett. **108**, 111804 (2012).
[105] S. Chatrchyan *et al.* (CMS Collaboration), Report No CMS-PAS-BTV-11-002, 2011.
[106] A. Abulencia *et al.* (CDF Collaboration), Phys. Rev. D **73**, 032003 (2006).
[107] S. Chatrchyan *et al.* (CMS Collaboration), Report No. CMS-PAS-EXO-11-051, 2011.
[108] S. Catani, L. Cieri, D. de Florian, G. Ferrera, and M. Grazzini, Phys. Rev. Lett. **108**, 072001 (2012),URL http://link.aps.org/doi/10.1103/PhysRevLett.108.072001.